Impact of Demand Response on Stability Region of Single-Area LFC System with Communication Delay

Saffet Ayasun[1] and Chika O. Nwankpa[2]

[1]Department of Electrical Engineering, Niğde Ömer Halisdemir University, Main Campus, 51240, Niğde Turkey
sayasun@ohu.edu.tr
[2] Department of Electrical and Computer Engineering, Drexel University, Philadelphia, 19104, US
chika@coe.drexel.edu

Abstract

This paper investigates the impact of dynamic demand response (DR) on the stability region depicted on the controller parameter space of a single-area load frequency control (LFC) system with communication time delays. An effective and simple graphical method is implemented to compute all stabilizing Proportional Integral (PI) controller gains of DR loop for a given time delay. The approach is based on extracting stability region and the stability boundary locus in the PI controller parameter space.

1. Introduction

The main goal of the conventional LFC system is to maintain a reasonably uniform frequency in an interconnected power system consisting of several pools. The system frequency is regulated by balancing generation and demand through load following [1]. On the other hand, renewable energy (RE) sources such as wind power, photovoltaic (PV) and fuel cells will have a considerable share of power generation as distributed generation sources in the future smart power grid [2], [3]. Therefore, conventional LFC systems get more complicated in terms of frequency regulation. Besides, highly variable generations such as wind power and PVs are unsatisfactory to maintain frequency at its desired value. Energy storage devices and responsive loads are essential for stability of future power grids and for balancing between load demands and power generations [3]-[6].

Due to disadvantages of the renewable energy such as the high costs, low efficiency, power fluctuation, variability and uncertainty of wind and solar resources, dynamic demand response (DR) which plays an important role in providing ancillary services on conventional power plants should be considered as an option in frequency regulation [7]. DR is designed to contribute to energy load reduction and stability of power grid during times of peak demand. When demand is high and supply is inadequate or is the opposite, frequency of interconnected power grid cannot be at its desired value. Additionally, DR increases reliability and flexibility of interconnected power systems, decreases the cost of operation, and enhances system efficiency. To avoid unwanted effects of renewable energy, conventional LFC system is modified using DR loop [8].

With the inclusion of the DDR loop and open communication network in the LFC system, inevitable time delays are observed. These delays include measurement and communication delays [8]. Traditionally, dedicated communication links were used to sending and receiving control signals. For this reason, in stability analysis it was reasonable to neglect time delays associated with the communication network. However, communication delays significantly increase when an open and distributed communication network is used to send control signals [9], [10]. It was reported that communication delays in LFC systems can be in the range of 5-15 sec [11]. The size of communication delays mainly depends on the physical media of communication (such as fiber-optic-cables, digital microwave links, power line, telephone lines and satellite links [9]) as well as several other factors including the phasor package size, transmission protocol employed and communication network load (congested or idle).

Time delays have become a great concern in stability analysis and controller design of LFC systems since these delays may destabilize the system and reduce the controller performance. Recent studies on the delay-dependent stability of LFC system mainly focus on the identification stability delay margin for a given set of PI controller parameters. They aims to compute delay values for which LFC systems will be marginally stable using frequency domain direct methods [12] or time domain indirect methods based on Lyapunov stability theory [13].

For a complete picture of the LFC system stability, it is also vital to determine all possible values of PI controller parameters that ensure a stable operation when a time delay is observed. In one of our earlier work reported in [14], a simple graphical technique that aims to compute stability boundary locus [15, 16] has been used to stability analysis of time-delayed single-area LFC system, and a stability region for a given time delay has been determined in the PI controller parameters space. This paper extends our earlier work on the stability region [14] to investigate the impact of DR loop on the stability regions. The proposed method has been effectively applied to controller design and synthesis of integrating systems containing time delays [17] and large wind turbine systems [18]. Stability regions are obtained for a wide range of communication time delays and the impact of DR is evaluated for different frequency regulation scenarios realized by a control effort sharing factor. The accuracy of theoretical delay margins is validated by using Matlab/Simulink [19] to demonstrate the effectiveness of the proposed method.

2. Modified LFC model with DR loop

Conventional LFC system is modified to include a DR loop as an ancillary service in addition to the supplementary control loop. Fig. 1 shows the block diagram of the modified LFC system. Observe that total time delays are lumped into a single

constant delay to simplify stability analysis and an exponential transfer function $e^{-s\tau}$ is introduced in both control loops. With the DR available in the LFC, the required control effort called Ω can be shared between supplementary and DR loops based on their cost at real-time electricity market as follows:

$$\begin{aligned}\Delta P_S(s) &= \alpha\Omega \\ \Delta P_{DR}(s) &= (1-\alpha)\Omega\end{aligned} \tag{1}$$

where α is a sharing factor $(0<\alpha<1)$ that determines weight of secondary control or DR control. The control effort $\alpha=1$ means that total required frequency regulation will be provided by the traditional secondary regulation services, i.e. spinning and non-spinning reserve, and $\alpha=0$ is the case where all the required control would be provided by DR. The decision on the values of (α) should be made by ISO/RTO, based on the price of DR and the traditional regulation services in a real-time market [8].

The variables $\Delta f, \Delta P_G, \Delta P_T,$ and ΔP_L in Fig. 1 represent the deviation of frequency, the generator mechanical output, valve position, and load, respectively. The system parameters H, D, T_g, T_t and R are the moment of inertia of the generator, generator damping coefficient, time constant of the governor, time constant of the turbine, and speed drop, respectively.

The characteristic equation needs to be determined to obtain stability regions of the LFC system with a DR loop.

$$\begin{aligned}&\Delta(s,\tau) = p_4 s^4 + p_3 s^3 + p_2 s^2 + p_1 s + \\ &\left(\begin{array}{l} K_P\left[q_3' s^3 + q_2' s^2 + q_1' s\right] + \\ K_I\left[q_2'' s^2 + q_1'' s + q_0''\right] + q_1 s + q_0 \end{array}\right) e^{-s\tau} = 0\end{aligned} \tag{2}$$

where $P(s)$ and $Q(s)$ are polynomials s with real coefficients and in terms of system parameters given below:

$$\begin{aligned}&p_4 = M.R.T_g.T_t, p_3 = M.R.T_g + M.R.T_t + D.R.T_g T_t, \\ &p_2 = M.R + D.R.T_g + D.R.T_t,\ p_1 = 1 + DR, \\ &q_3' = RT_g T_t(1-\alpha), q_2' = RT_g(1-\alpha) + RT_t(1-\alpha) \\ &q_2'' = RT_g T_t(1-\alpha), q_1 = K_{PS} R\alpha \\ &q_1' = R(1-\alpha), q_1'' = RT_g(1-\alpha) + K_I RT_t(1-\alpha); \\ &q_0 = K_{IS} R\alpha, q_0'' = R(1-\alpha)\end{aligned}$$

Note that secondary control and DR loops are assumed to have different PI controller gains so that impact of DR controller loop could be appropriately assessed. As shown in Fig. 1, (K_{PS}, K_{IS}) represent PI controller gains of the secondary control loop while (K_P, K_I) denote those of the DR control loop. It must be stated that (K_{PS}, K_{IS}) are tuned and fixed by the utility as to have desired frequency response without considering the DR control loop.

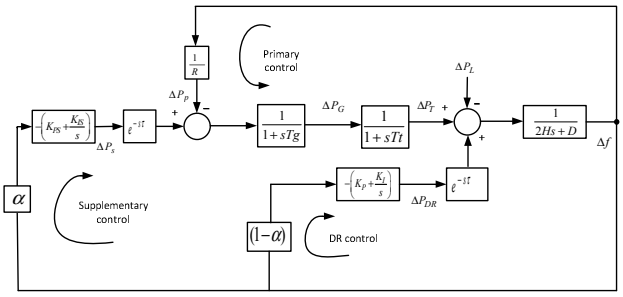

Fig. 1. Block-diagram representation of single area-LFC system model with a DR control loop

3. Computation of stability regions

To identify the boundary of the stability region for a given time delay τ, we substitute $s=j\omega$ with $\omega>0$ and $e^{-j\omega\tau} = \cos(\omega\tau) - j\sin(\omega\tau)$ into the characteristic equation of (2) as follows:

$$\begin{aligned}&\Delta(s,\tau) = p_4(j\omega)^4 + p_3(j\omega)^3 + p_2(j\omega)^2 + p_1(j\omega) + \\ &\left(\begin{array}{l} K_P\left[q_3'(j\omega)^3 + q_2'(j\omega)^2 + q_1'(j\omega)\right] + \\ K_I\left[q_2''(j\omega)^2 + q_1''(j\omega) + q_0''\right] + \\ q_1(j\omega) + q_0 \end{array}\right)\left(\cos(\omega\tau) - j\sin(\omega\tau)\right) = 0\end{aligned} \tag{3}$$

Separating into the real and imaginary parts, we get a more compact form of (3) as

$$\begin{aligned}&K_P A_1(\omega) + K_I B_1(\omega) + C_1(\omega) + \\ &j\left(K_P A_2(\omega) + K_I B_2(\omega) + C_2(\omega)\right) = 0\end{aligned} \tag{4}$$

Setting both real and imaginary parts of (4) to zero, we get

$$\begin{aligned}K_P A_1(\omega) + K_I B_1(\omega) + C_1(\omega) &= 0 \\ K_P A_2(\omega) + K_I B_2(\omega) + C_2(\omega) &= 0\end{aligned} \tag{5}$$

The expressions for A_1, B_1, C_1, A_2, B_2, and C_2 are as follows:

$$\begin{aligned}A_1(\omega) &= q_1'\omega\sin(\omega\tau) - q_2'\omega^2\cos(\omega\tau) - q_3'\omega^3\sin(\omega\tau) \\ B_1(\omega) &= -q_2''\omega^2\cos(\omega\tau) + q_0''\cos(\omega\tau) + q_1''\omega\sin(\omega\tau) \\ C_1(\omega) &= p_4\omega^4 - p_2\omega^2 + q_0\cos(\omega\tau) + q_1\omega\sin(\omega\tau) \\ A_2(\omega) &= -q_3'\omega^3\cos(\omega\tau) + q_2'\omega^2\sin(\omega\tau) + q_1'\omega\cos(\omega\tau) \\ B_2(\omega) &= q_2''\omega^2\sin(\omega\tau) + q_1''\omega\cos(\omega\tau) - q_0''\sin(\omega\tau) \\ C_2(\omega) &= -p_3\omega^3 + p_1\omega + q_1\omega\cos(\omega\tau) - q_0\sin(\omega\tau)\end{aligned} \tag{6}$$

We then solve (5) for (K_P, K_I) to identify the stability boundary locus $\ell(K_P, K_I, \omega)$ in the (K_P, K_I)-plane.

$$\begin{aligned}K_P &= \frac{B_1(\omega)C_2(\omega) - B_2(\omega)C_1(\omega)}{A_1(\omega)B_2(\omega) - B_1(\omega)A_2(\omega)} \\ K_I &= \frac{A_2(\omega)C_1(\omega) - A_1(\omega)C_2(\omega)}{A_1(\omega)B_2(\omega) - B_1(\omega)A_2(\omega)}\end{aligned} \tag{7}$$

This boundary locus represents a set of PI controller gains of DR loop for which the characteristic equation of (2) a pair of complex conjugate roots, $s = \pm j\omega$ with $\omega > 0$, on the imaginary axis for a given time delay. The stability exchange occurs due to root crossing of the imaginary axis not including the origin. Such a boundary locus is defined as the Complex Root Boundary (CRB) of the stability region since the resulting instability is an oscillatory instability situation [15, 16].

It is also possible that instability may when a real root of (2) moves from the negative left-half plane to the positive one thru the origin, $s = j\omega = 0$ as the controller gains vary. Substituting $s = j\omega = 0$ into (3) we obtain the following condition for the root crossing thru the origin.

$$K_I q_0'' + q_0 = 0$$
$$K_I = -\frac{q_0}{q_0''} = -\frac{K_{IS}\alpha}{(1-\alpha)} \tag{8}$$

The boundary locus in (8) is known as Real Root Boundary (RRB) locus [15, 16]. Consequently, the CRB locus, $\ell(K_{PC}, K_{IC}, \omega_c)$ in (7) and the RRB locus in (8) constitute the stability boundary locus and split (K_P, K_I)-plane into stable and unstable regions.

4. Results

The section presents stability regions and verification studies using time-domain simulations. The parameters of the single-area LFC system are as follows [8]:

$$2H = 0.1667,\ T_g = 0.08\ s,\ T_t = 0.4s, R = 3,$$
$$D = 0.015, K_{PS} = 0.05, K_{IS} = 0.05$$

It has been reported that maximum time delay in the DR loop is around $\tau = 0.5\ s$ [4, 8]. Therefore, time delay is chosen as $\tau = 0.5\ s$ and stability region is obtained using (7) and (8) for the sharing factor of $\alpha = 0.8$. The boundary of stability region shown in Fig. 3 consists of CRB and RRB locus defined by (7) and (8). This region provides a set of DR controller gains for which the LFC system will be stable. Time domain simulations are performed to illustrate the stability exchanges due to the crossing of CRB or RRB locus. Fig. 4 shows the frequency responses of the LFC system with three different DR controller gains. It is clear that the system is marginally stable when the controller gains are on the CRB locus, $(K_P = 1.533, K_I = 1.501)$ as shown in Fig. 3. On the other hand, Fig. 4 clearly indicates the system exhibits oscillatory instability (growing oscillations) for the controller gain outside of the stability region, $(K_P = 1.533, K_I = 1.55)$ and oscillatory stability (decaying oscillations) for the PI gains inside the region, $(K_P = 1.533, K_I = 1.40)$. This instability is observed to the crossing of CRB locus.

Note that the RRB is found as $K_I = -0.2$ using (8) for $K_{IS} = 0.05, \alpha = 0.8$. The DR loop controller gains are chosen as $K_P = 0.5, K_I = -0.25$ to the left of $K_I = -0.2$ vertical line to illustrate the exponential instability. Fig. 4 clearly presents exponential instability due to the crossing of the RRB locus.

Stability regions are obtained for various values of the sharing factor α to illustrate the impact of the DR loop on the shape and size of the regions. Fig. 5 shows stability regions for a range of the sharing factor, $\alpha = 0.2 - 0.8$ when the delay is fixed at $\tau = 0.5\ s$. Recall that α is the sharing factor $(0 < \alpha < 1)$ that determines weight of secondary control and DR control loops. Fig. 5 clearly illustrates that the size of regions is getting bigger as the share of the secondary control loop increases (or the share of the DR loop decreases) resulting in a large set of DR controller gains.

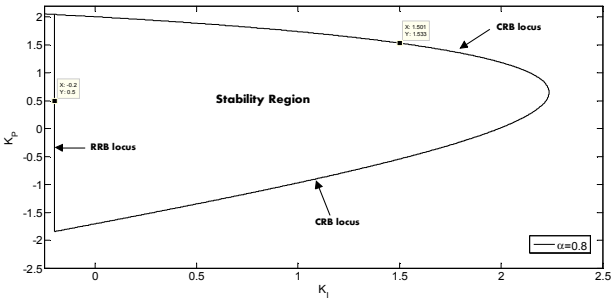

Fig. 2. Stability region with CRB and RRB locus for $\alpha = 0.8, \tau = 0.5\ s$.

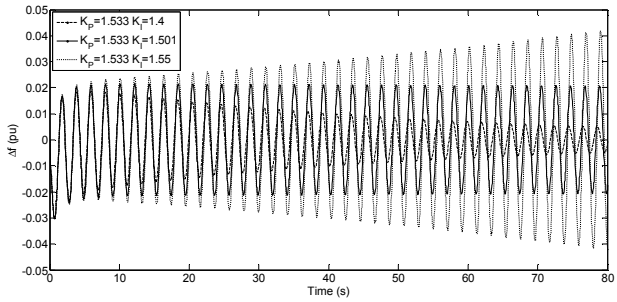

Fig. 3. Frequency response illustrating oscillatory instability for different DR loop controller gains around the CRB when $\alpha = 0.8, \tau = 0.5\ s$

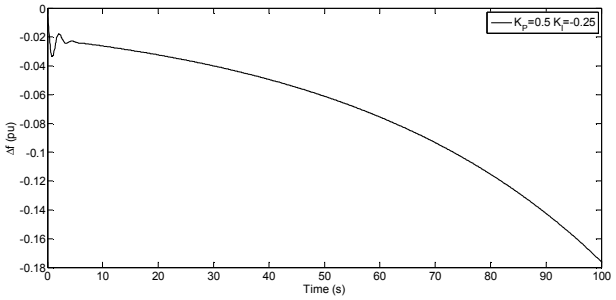

Fig. 4. Frequency response illustrating exponential instability for $\alpha = 0.8, \tau = 0.5\ s$

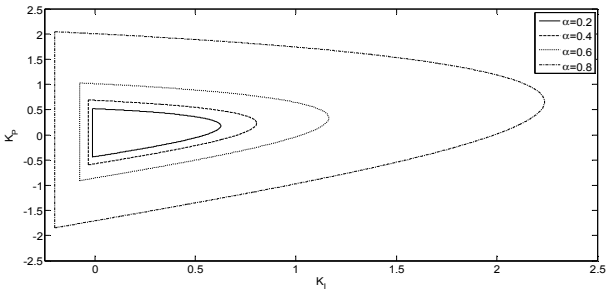

Fig. 5. Stability regions for various α values when $\tau = 0.5\ s$

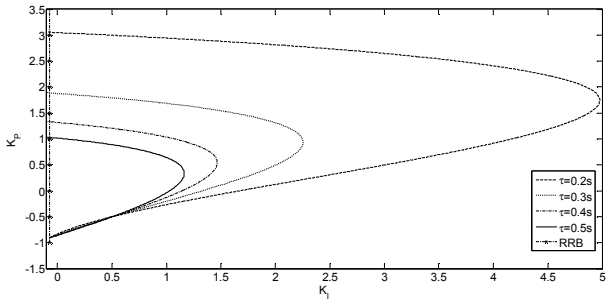

Fig. 6. Effect of time delay on the stability regions for $\alpha = 0.6$

6. Conclusions

This paper has utilized an analytical graphical method to obtain stability regions in the DR controller gain space and to investigate the impact of DR loop on the frequency regulation Results indicate that stability regions become smaller as the sharing portion of the DR control loop increases due to the existence of a time delay in the DR loop. Moreover, increase in time delay causes a smaller region for a chosen scenario of control effort sharing. In order to efficiently integrate the DR loop into frequency regulation, one needs to perform a trade-off study between the control effort contribution of the DR loop and time delay observed in the loop.

7. Acknowledgment

This work was supported by International Postdoctoral Research Scholarship Programme of the Scientific and Technological Research Council of Turkey under the Project 1M056 1059B191600680.

8. References

[1] P. Kundur, "Power System Stability and Control", New York: McGraw-Hill, 1994.

[2] U.S. Department of Energy Smart Grid, http://energy.gov/oe/technology-development/smart-grid, accessed June 2016.

[3] C. W. Gellings, *The smart grid: Enabling energy efficiency and demand response*, CRC Press, 2009.

[4] A. Brooks, E. Lu, D. Reicher, et al., "Demand dispatch: Using real-time control of demand to help balance generation and load," *IEEE Power Energy Mag.*, vol. 8, no. 3, pp. 20–29, 2010.

[5] M. Muthalib and C. O. Nwankpa, "Incorporating dynamic building load model into interconnected power systems," in *Proc. of Innovative Smart Grid Technologies (ISGT) IEEE PES*, Washington, DC, Feb. 2013, pp. 1-6.

[6] K. Samarakoon, J. Ekanayake, and Jenkins, "Investigation of domestic load control to provide primary frequency response using smart meters," *IEEE Trans. Smart Grid*, vol. 2, no. 1, pp. 282–292, 2012.

[7] S. A. Pourmousavi, M. H. Nehrir, and C. Sastry, "Providing ancillary services through demand response with minimum load manipulation," in *Proc. North Amer. Power Symp. (NAPS),* Boston, MA, Aug. 2011, pp. 1-6.

[8] S. A. Pourmousavi and M. H. Nehrir, "Introducing dynamic demand response in the LFC Model," *IEEE Trans. Power Syst.*, vol. 29, no. 4, pp. 1562-1572, 2014.

[9] B. Naduvathuparambil, M. C. Valenti, and A. Feliachi, "Communication delays in wide area measurement systems," in *Proc. the 34th Southeastern Symposium on System Theory (SSST2002),* Huntsville, Alabama, March 18-19, 2002, pp. 118-122.

[10] X. Yu and K. Tomsovic, "Application of linear matrix inequalities for load frequency control with communication delays," *IEEE Trans. Power Syst.*, vol. 19, vol. 3, pp. 1508-1515, 2004.

[11] M. Liu, L. Yang, D. Gan, D. Wang, F. Gao, and Y. Chen, "The stability of AGC systems with commensurate delays," *Euro. Trans. Electr. Power,* vol. 17, no. 6, pp. 615-627, 2007.

[12] Ş. Sönmez, S. Ayasun, C.O. Nwankpa, "An exact method for computing delay margin for stability of load frequency control systems with constant communication delays," *IEEE Trans. Power Syst.*, vol. 31, no. 1, pp. 370-377, 2016.

[13] L. Jiang, W. Yao, Q. H. Wu, et al., "Delay-dependent stability for load frequency control with constant and time-varying delays," *IEEE Trans. Power Syst.*, vol. 27, no. 2, pp. 932-941, 2012.

[14] Ş. Sönmez and S. Ayasun, "Stability region in the parameter space of PI controller for a single-area load frequency control system with time delay," *IEEE Trans. Power Syst.*, vol. 31, no.1, pp. 829-830, 2016.

[15] M. T. Söylemez, N. Munro, and H. Baki, "Fast calculation of stabilizing PID controller," *Automatica*, vol. 39, no. 1, pp. 121–126, 2003.

[16] N. Tan, I. Kaya, Yeroglu, C., et al., "Computation of stabilizing PI and PID controllers using the stability boundary locus," *Energy Conversion and Management*, vol. 47, pp. 3045-3058, 2006.

[17] S. E. Hamamcı and M. Köksal, "Calculation of all stabilizing fractional-order PD controllers for integrating time delays," *Computers and Mathematics with Applications*, vol. 59, pp. 1621-1629, 2010.

[18] J. Wang, N. Tse, and Z. Gao, "Synthesis on-PI-based pitch controller of large wind turbine generator," Energy Conversion and Management, vol. 52, no. 2, pp. 1288-1294, 2011.

[19] Simulink: *Model-Based and System-Based Design, Using Simulink*, MathWorks Inc., Natick, MA, 2000.